Published in final edited form as:
Dev Biol. 2007 September 15; 309(2): 373–385.

A zebrafish LMO4 ortholog limits the size of the forebrain and eyes through negative regulation of *six3b* and *rx3*

Catherine W. McCollum, **Shivas R. Amin**, **Philip Pauerstein**, and **Mary Ellen Lane***
Department of Biochemistry and Cell Biology, Rice University, Houston Texas 77005

Abstract

The Six3 and Rx3 homeodomain proteins are essential for the specification and proliferation of forebrain and retinal precursor cells of the vertebrate brain, and the regulatory networks that control their expression are beginning to be elucidated. We identify the zebrafish *lmo4b* gene as a negative regulator of forebrain growth that acts via restriction of *six3* and *rx3* expression during early segmentation stages. Loss of *lmo4b* by morpholino knockdown results in enlargement of the presumptive telencephalon and optic vesicles and an expansion of the post-gastrula expression domains of *six3* and *rx3*. Overexpression of *lmo4b* by mRNA injection causes complementary phenotypes, including a reduction in the amount of anterior neural tissue, especially in the telencephalic, optic and hypothalamic primordia, and a dosage-sensitive reduction in *six3* and *rx3* expression. We suggest that *lmo4b* activity is required at the neural boundary to restrict *six3b* expression, and later within the neural plate to for attenuation of *rx3* expression independently of its effect on *six3* transcription. We propose that *lmo4b* has an essential role in forebrain development as a modulator of *six3* and *rx3* expression, and thus indirectly influences neural cell fate commitment, cell proliferation and tissue growth in the anterior CNS.

Keywords

zebrafish; LMO4; boundary; telencephalon; eye; cell proliferation; six3; rx3

Introduction

In zebrafish embryos, the size of the anterior neural plate, and the position of the neural-non-neural boundary are determined during gastrulation, through the activity of the Wnt and Bmp pathways (Rhinn et al., 2006; Wilson and Houart, 2004). The activity of both pathways is hypothesized to be graded throughout the ectoderm, and an early outcome of graded activities is differential expression of selector genes for anterior neural fate commitment. The *six3* gene encodes a homeodomain transcription factor that positively regulates neural cell fate commitment and growth of anterior tissue in all vertebrates studied. Mouse embryos deficient for *six3* function have severe forebrain and eye defects (Lagutin et al., 2001; Lagutin et al., 2003). Morpholino depletion of *six3* in Xenopus (Gestri et al., 2005) or Medaka fish (Carl et al., 2002; Del Bene et al., 2004) or expression of a dominant-negative *six3* in Xenopus (Gestri et al., 2005) or zebrafish (Kobayashi et al., 2001) results in similar defects. Overexpression analyses (Kobayashi et al., 2001; Loosli et al., 1999; Lopez-Rios et al., 2003; Zuber et al., 2003) have further elucidated the mechanism of *six3* activity. Briefly, vertebrate *Six3* acts as

*Corresponding author: melane@rice.edu; 713 348 5254 (phone) 713 348 5154 (fax).

a transcriptional repressor that maintains the low BMP activity levels that permit specification of anterior neuroectoderm, promotes cell proliferation and delays neurogenesis in the anterior neuroectoderm (Gestri et al., 2005). Six3 binds directly to the *bmp4* promoter (Gestri et al., 2005) and Six3 regulates expression of critical cell cycle genes to promote cell proliferation. An additional non-transcriptional mechanism has been demonstrated for *Six3*-dependent proliferation. *Six3* binds Geminin, a negative regulator of DNA replication initiation, thus allowing DNA replication to initiate (Del Bene et al., 2004).

The *rx3* gene is essential for eye development in fish (Chuang et al., 1999; Kennedy et al., 2004; Loosli et al., 2003; Loosli et al., 2001; Rembold et al., 2006; Rojas-Munoz et al., 2005; Stigloher et al., 2006). This homeodomain transcription factor is expressed in the eye field during and after gastrulation, and permits eye development by blocking telencephalon specification (Stigloher et al., 2006) and promoting proliferation and morphogenesis of the optic precursors (Bailey et al., 2004; Kennedy et al., 2004; Loosli et al., 2001; Mathers and Jamrich, 2000; Rembold et al., 2006). The mechanisms by which *rx* activity leads to enhanced cell proliferation are not well understood, however transcriptional regulation of rate limiting cell cycle factors has been proposed (Andreazzoli et al., 2003; Bailey et al., 2004; Casarosa et al., 2003).

We have previously identified a zebrafish ortholog of the mammalian proto-oncogene *Lmo4* that is expressed dynamically at the border of the anterior neural plate, and in the developing forebrain and optic primordia (Lane et al., 2002; Sagerstrom et al., 2001). Several members of the LMO family of transcriptional regulators are implicated in the regulation of cell fate specification, boundary formation and proliferation control in Drosophila and vertebrates. Lmo4, in particular, has roles in generating neuronal diversity, promoting neural tube closure and promoting proliferation in mammary duct tissue (Visvader et al., 2001; Manetopoulos et al., 2003; Hahm et al., 2004; Tse et al., 2004; Wang et al., 2004; Lee et al., 2005;Sum et al., 2005b). We show here that zebrafish *lmo4b* has essential and unanticipated roles in anterior CNS development. Morpholino-induced loss of *lmo4b* results in enlargement of the forebrain and optic vesicles, whereas global misexpression of *lmo4b* has the opposite effect. Our results suggest that *six3* and *rx3* are independently negatively regulated by Lmo4b, and that Lmo4b is a component of the regulatory network that stabilizes the anterior neural boundary and ensures the appropriate subdivision of regional cell fates within the anterior neural plate.

Materials and Methods

Fish husbandry

Zebrafish (*Danio rerio*) were maintained at 28.5°C as described in Westerfield (1994). Embryos were collected from natural mating and staged according to Kimmel et al. (1995).

Plasmid construction

The *lmo4b* coding region was amplified from full-length cDNA (Lane et al., 2002) and cloned into pCS2+MT vector to generate *pCS2+-myc-lmo4b*. For morpholino efficiency studies, a PCR-amplified region containing 100 bp of the *lmo4b* 5′ UTR and the entire coding region was inserted into pCS2+MT vector to generate *pCS2+5′UTR-lmo4b-myc*. Injection of in vitro transcribed mRNA was assayed for the ability to phenocopy injection of un-tagged *lmo4b* mRNA and for nuclear anti-Myc immunoreactivity.

RNA injection

Capped sense RNA was synthesized using the mMESSAGE mMACHINE kit (Ambion) from *pCS2+myc-lmo4b* and *pCS2+5′UTR-lmo4b-myc*. Microinjections were carried out using the Harvard Apparatus PLI-90 microinjector. For double mRNA injections and mRNA-MO

injections, embryos were injected separately with 4nl of each mRNA at the appropriate concentration. For double mRNA injections, GFP mRNA was used in single overexpression experiments to standardize the amount of nucleic acid injected into each embryo.

Morpholino injection

Antisense morpholino oligonucleotides against *lmo4b* mRNA were designed and synthesized by Gene Tools, LLC. The sequences of the two non-overlapping translational blocking *lmo4b* MOs were 5′-CTGTTCACCATCGCCTGCCGTTATT-3′ (−14 to 11, using the first nucleotide of the start codon as the reference) and 5′-ACGTATCTCGAAGGTCAAAGGGTGC-3′ (−42 to −18). The sequence of the mismatched control MO for *lmo4b* containing 4 base substitutions (in lower case) was 5′-CTGaTCAgCATCGCCTGCgGTTtTT-3′ (−14 to 11). The dosage for morpholino injection was 4 or 5 ng per embryo.

Western blot

For morpholino efficiency studies, each embryo was injected with 750 pg of *5′UTR-lmo4b-myc* mRNA, followed by injection of translational blocking *lmo4b* MOs at 3 ng, 6 ng, or 9 ng. Animal caps from injected and uninjected wild-type embryos were obtained at approximately 3.5 hpf as described (Grinblat 1999), and resuspended in 2X Laemmli buffer. Half of the protein samples generated from the animal caps were loaded onto a 12% SDS-PAGE gel and separated by electrophoresis. The presence of myc-tagged Lmo4b protein was detected with monoclonal mouse α-myc antibody (1:10,000) and peroxidase-conjugated goat-α-mouse antibody (1:50,000) using enhanced chemiluminescence (Amersham Biosciences).

Whole-mount in situ hybridization

All procedures for whole-mount in situ hybridization were carried out as described (Sagerström et al., 1996). The clones used for this study have been previously described: *lmo4b* (Lane et al., 2002), *pax2a* (Krauss et al., 1991) *pax6b* (Nornes et al., 1998) *rx2/3* (Mathers et al., 1997), *emx1* (Morita et al., 1995) *dlx3* (Akimenko et al., 1994) *six3b* (Seo et al., 1998) *zic1* (Grinblat et al., 1998), *shh* (Schauerte et al., 1998), and nk2.1a (Rohr and Concha, 2002). For double in situ hybridization, the staining of the fluoresceinated probe was developed in the presence of INT (Boehringer) and BCIP (Sigma) to give an orange precipitate or with BCIP and Fast Red tablets (Roche), to give a light blue precipitate (Hurtado and Mikawa, 2006). Images were obtained using the Zeiss Axioskop II Plus microscope and a Zeiss AxioCam MRc camera and processed in Adobe Photoshop. Sections were hand-cut with a razor blade.

Measurement of morphant heads

To quantitatively estimate the head-specific defects in *lmo4b* knockdown embryos, 4 ng of *lmo4b* MO cocktail or of 4mmMO were injected per embryo and measurements were obtained at the 10-somite stage. We measured the dorsoventral head height through the center of the optic vesicle, from yolk to the top of the head. We also measured the diameter of the optic vesicle along the nasotemporal axis, through the center of the vesicle. For both injection groups, n=20 embryos. These calculations were performed as described in Ando (2005). The averages, standard deviations and standard errors were determined, and significant differences were determined based on *p* values and confidence intervals. We measured yolk diameter from three points for each embryo to estimate the variability due to fixation, and found no significant variation.

The measurements shown in Figure 4 were obtained as follows: Embryos were deyolked and flat-mounted laterally, and viewed under the 20X objective. Regions a–d were taken as described in the text, using the “measure length” function in AxioVision LE, version 4.5.0.0

(Zeiss Imaging Solutions, 2005), and were converted from pixels to microns based on calibrated settings for the magnification and the microscope. Ratios of a/d, b/d, and c/d in control and morpholino-injected groups of embryos were compared using a t-test.

Results

Lmo4b functions in zebrafish brain, eye, ear and pectoral fin development

We previously described the cloning, expression and phylogeny of a zebrafish *lmo4* gene (Lane et al., 2002). We classified that gene as *lmo4* based on similar N- and C-terminal sequences. We have identified a second zebrafish gene from the Genbank database (Accession #AF398515). This gene has greater homology with mammalian *Lmo4*, and we designate this gene *lmo4a*. Our previously characterized gene, now designated *lmo4b*, has unique residues at positions otherwise highly conserved between zebrafish *lmo4a* and other mammalian Lmo4 genes, indicating potentially novel function (Fig. 1A, in red). We will present our analysis of the co-ortholog *lmo4a* elsewhere (S. Amin and M.E. Lane, in preparation).

To determine the function of *lmo4b*, we performed morpholino knock-down experiments with two translation-blocking morpholinos that target non-overlapping regions of the 5′ UTR (*lmo4b*-MO). *lmo4b* morphant embryos showed full axial elongation at 3 days post fertilization (dpf) compared with control embryos, with abnormalities in the head and eyes (Figs. 1C–F), ears (Figs. 1G and H) and pectoral fins (Figs. 1I and J). We have documented *lmo4b* expression in all affected tissues (Lane et al., 2002). As a control, we injected a morpholino containing 4-bp mismatched sequence (4mm-MO; Figs. 1C, E, G and I). In all further experiments, with the exception of those in Figure 7, we compare embryos injected with *lmo4b*-MO (referred to as “morphant embryos”) to embryos injected with 4mm-MO (referred to as “control embryos”).

We tested the efficiency and the specificity of *lmo4b* morpholinos by determining their ability to block translation of protein from exogenous mRNA that contains the MO target sequences in the 5′ UTR, followed by the *lmo4b* open reading frame fused to a C-terminal 6x-MYC tag. Embryos were first injected with mRNA, followed by injection with either the *lmo4b-MO* cocktail, or the 4mm-MO. In immunoblots, the 45kD exogenous *Lmo4b*-MYC band was significantly reduced in extracts from embryos injected with mRNA and *lmo4b*-MO, when compared with extracts from embryos injected with mRNA and the 4mm-MO (Fig. 1B).

Loss of *lmo4b* results in enlargement of forebrain and optic primordia by mid-segmentation stages

We examined younger embryos by morphology and in situ hybridization to determine when the anterior defects were first detectable. By the 10-somite (10s) stage, morphant embryos had enlarged heads relative to control-injected embryos in the optic and preoptic regions (Figs. 2A and B), while little or no morphological differences were apparent in more posterior regions. Injection of a splice-blocking MO that specifically targets zygotic transcripts produced embryos that were phenotypically similar to translation-blocked morphants (not shown). However, the splice blocking morpholino frequently produced off-targeting effects, including early necrosis in the brain and eyes, therefore all experiments presented here utilized translation-blocking morpholinos. Measurements of head height (HH) and eye diameter (ED) for embryos at the 10s stage, in the positions indicated by the lines in Figures 2A and 2B, revealed a significant difference between morphant and control embryos (Fig. 2C; $p=8.7\times10^{-5}$ for HH, $p=2.2\times10^{-5}$ for ED). Morphant heads were 24% larger than control-injected embryos and morphant eyes were 31% larger than those of control-injected embryos.

The *zic1*-expressing regions of the telencephalon and diencephalon were enlarged in both lateral (Figs. 2D and E) and dorsal (Figs. 2F and G) views. The optic vesicles were expanded

nasotemporally and mediolaterally, as visualized in dorsal views by morphology and *pax6b* expression (Figs. 2H and I). Expression of *pax2a* (blue in Fig. 2J and K) at the prim-5 stage (24 hours post fertilization) revealed an enlarged optic stalk and an indistinct boundary between the retina and optic stalk, with significant *pax2a* expression in cells that resemble presumptive retinal cells by their elongated morphology and *pax6b* expression (red in Figs. 2J and K). We also note the expanded preoptic area in morphant embryos (dashed line in Figs. 2L and M), consistent with the forebrain enlargement seen earlier. Additionally, we observed an enlarged hypothalamus, visualized by ventral views of *nk2.1a* expression at 28 hpf (the prim-6 stage; Figs. 2N and O). No regional differences were revealed upon staining for expression of *shh* and *emx1*, which are expressed in the dorsoanterior and posterioventral hypothalamus, respectively (not shown).

Loss of *lmo4b* does not disrupt early dorsoventral patterning or axial morphogenesis

We previously documented *lmo4b* expression prior to the midblastula transition, followed by dynamic zygotic expression near the shield stage. Expression in the anterior neural region is initiated after epiboly and persists throughout the segmentation period. To determine whether the forebrain enlargement results from loss of *lmo4b* activity specifically in anterior neural tissue, we addressed whether forebrain enlargement results secondarily from morphogenetic abnormalities in the neural tube or from early disruption of dorsoventral patterning or neural convergence. A requirement for *Lmo4* in mammalian anterior neural closure has been proposed based on the variable exencephaly observed in embryos in which *Lmo4* has been inactivated (Lee et al., 2005). In contrast, sections through the presumptive zebrafish forebrain, marked by *zic1* expression at the 10s stage, showed that neural keel morphogenesis is not disrupted (Figs. 3A and B). While morphants have more *zic1* expressing cells along the dorsoventral axis of the neural rod compared with control embryos, in both cases a single dorsal domain of expression indicated complete closure of the medial regions of the neural rod. Similarly, at 24 hpf, morphant embryos were not obviously distinguishable from control-injected embryos by morphology of the dorsoanterior neural tube, marked by *emx1* expression, or degree of neural tube closure (Figs. 3C and D).

To address early dorsoventral patterning and neural convergence, which could potentially be altered by loss of maternal, but not zygotic *lmo4b*, we compared the size of the neural plate at the end of gastrulation in morphant and control embryos by in situ hybridization with probes against the *dlx3b*, *shh* and *pax2a* genes. The distribution of these transcripts indicates whether the boundary between the neural plate and non-neural ectoderm is mispositioned, and whether the neural plate is larger in either its anteroposterior or mediolateral dimensions. We show in Figures 3E and 3F that the dorsal neuroectoderm of morphant embryos is of comparable size with control embryos at the bud stage. Measurements of the mediolateral width of the *pax2a* domain revealed no significant differences between morphant and control embryos (not shown). We conclude that loss of *lmo4b* does not disrupt patterning or morphogenesis of the anterior neural plate prior to the end of gastrulation, and that neural tube closure does not require *lmo4b* activity in zebrafish embryos.

Anterior neural expansion in *lmo4b* morphants results from disruption of the anterior neural boundary

To characterize the regional nature of the forebrain expansion, we measured and compared the anteroposterior length of the presumptive brain subdivisions at the 10s stage, as demarcated by a mixture of in situ probes hybridization for anterior neural genes (Figs. 4A–C). The *zic1* gene is expressed in the telencephalon and diencephalon. The *pax2a* gene is expressed at the presumptive midhindbrain boundary (MHB) and *krox20* is expressed in the presumptive third (r3) and fifth rhombomeres (r5) of the hindbrain. The telencephalon and diencephalon (region **a**) are demarcated by the *zic1* domain. The midbrain (region **b**) is demarcated by the caudal

edge of the *zic1* domain to the rostral edge of the *pax2a* domain. The rostral hindbrain (region **c**) is demarcated by the caudal edge of the *pax2a* domain to the rostral edge of the first *krox20* stripe. We previously showed that *lmo4b* is expressed in the rostral hindbrain during gastrulation and early segmentation stages (Lane et al., 2002). Finally, the region extending from the rostral end of the presumptive r3 to the caudal end of the presumptive r5 (region **d)** was measured to normalize for size variation that is independent of *lmo4b* function, as *lmo4b* is not expressed in this region at any time; therefore no changes are expected to result from loss of *lmo4b*, and indeed values for this measurement did not vary significantly between morphant and control embryos (p=0.06). The normalized values are shown as relative units in Figure 4C. We observed a statistically significant change in the length of the telencephalon and diencephalon (region a; p =0.009), and no significant differences in the length of either the midbrain (region b; p =0.7) or the rostral hindbrain (region c; p=0.055). We conclude that the expansion of the forebrain does not occur at the expense of more caudal neural tissue. We hypothesized therefore that loss of *lmo4b* expands anterior neural tissue by increased recruitment of cells at the anterior neural boundary, or by increased cell proliferation, or through both mechanisms.

To test whether loss of *lmo4b* leads to more recruitment of cells into anterior neural tissue after gastrulation, we determined when anterior neural expression of *lmo4b* is first visible by in situ hybridization. At the bud-1s stage, we saw *lmo4b* expression in a region overlapping with the anterior edge of the *zic1* expression domain (Fig. 4D, and enlarged view to show overlap in Fig. 4E). Expression of *lmo4b* is generally seen in 4–5 cells at the boundary between the neural plate (np) and the non-neural ectoderm (nne) (Fig. 4F). By the 3s stage, *lmo4b* expression is in the boundary region and largely excluded from the anterior neural plate, as seen in a cross section through the anterior neural region (arrow in Fig. 4G). Non-neural expression remains visible in cross sections through the anterior neural region at the 6s stage (arrow in Fig. 4H), but by this stage *lmo4b* is also expressed at within the neural keel (Fig. 4H). We conclude that the anterior domain of *lmo4b* initially overlaps with anterior neural genes in cells that ultimately segregate with the non-neural ectoderm, and thus may have a role in the refinement of gene expression at the neural boundary.

To further test the hypothesis that loss of *lmo4b* expands anterior neural tissue by permitting more boundary cells to adopt a neural fate, we next determined whether *zic1* expression was expanded after the 1s stage. We observed a larger area of *zic1* expression in *lmo4b* morphants (Figs. 4I and J), suggesting that the absence of *lmo4b* from the boundary region results in expansion or persistence of *zic1* expression. The results of *lmo4b* overexpression support this interpretation, as the domain of the *zic1* expression is diminished at the 2s stage (Fig. 4K). We conclude that *lmo4b* function is required in the neural boundary region during early somite stages to attenuate anterior neural gene expression in the cells at the presumptive boundary, thus limiting the number of cells that stably adopt a neural fate.

Lmo4b negatively regulates expression of *six3b* and *rx3* in the forebain and eye primordia in a dosage sensitive manner

The enlarged telencephalon, diencephalon, retina and optic stalk of *lmo4b* morphants is similar to the phenotype described for overexpression of the *six3* genes in zebrafish (Kobayashi et al., 1998) and Xenopus (Gestri et al., 2005), suggesting *six3* and *lmo4b* have opposite activities on the same process. In agreement with this, a similar domain of overlapping expression was seen for *lmo4b* and *six3b* at the 1s stage (not shown), and importantly, *lmo4b* morphant embryos have an enlarged *six3b* expression domain (Fig. 5A) compared with control embryos at the 3s stage (Fig. 5C), suggesting that *six3b* transcription is negatively regulated directly or indirectly by *lmo4b*. Similarly, when we overexpressed *lmo4b* by injection of 300 pg or 750 pg of *lmo4b* mRNA, we see that the *six3b* expression domain is reduced (Figs. 5D and E,

respectively). Overexpression experiments suggested that the effect of increased and decreased *lmo4b* activity on *six3b* expression was dosage sensitive. We confirmed this possibility by injection of lower amounts of morpholino (2ng; Fig. 5B), which produced a weaker effect than injection of high amounts (4ng Fig. 5A).

We then determined whether expression of the *rx3* gene, which directs proliferation and behavior of cells in the optic primordia, was also affected by *lmo4b* dosage. We observed a similar dosage-dependent effect as was seen for *six3b* (Figs. 5F–J). The increase in the expression domains for *six3b* and *rx3* are consistent with our proposed role for increased recruitment of ectodermal cells into the telencephalic and optic fields.

Loss of *lmo4b* results in increased number of proliferating cells in the optic vesicles

Given the important roles for *six3* and *rx3* in promoting cell proliferation and specification in the forebrain and eye (Bailey et al., 2004; Carl et al., 2002; Del Bene et al., 2004; Gestri et al., 2005; Stigloher et al., 2006), it is also possible that increased proliferation in the forebrain and eye contribute to the expansion of these regions in *lmo4b* morphants. To test this possibility we determined both the number of mitotic cells and the proportion of mitotic cells in the optic vesicles of *lmo4b* morphant and control embryos to quantify effects of loss of *lmo4b* on cell proliferation. We chose embryos at the 7s stage, at which time high expression of *lmo4b* occurs in anterior neural tissue, and all morphant embryos clearly show enlarged anterior neural primordia by both morphology and gene expression. Also, this time point is approximately two hours later than the appearance of increased *six3b* and *rx3* mRNA, and we assumed sufficient protein would have accumulated to produce an effect on cell proliferation.

We stained embryos for mitotic nuclei with antibodies against phospho-histone H3 (anti-PH3), and counterstained with Hoescht 3258 to reveal all nuclei. PH3-positive cells and total cell numbers were determined for the telencephalon and optic vesicles from 10μ optical sections of morphant and control embryos. We observed a significant increase in the average number of mitotic cells in the optic vesicles of *lmo4b* morphants at the 7s stage (Figs. 6C, D and F; $p=1.9\times10^{-4}$). At this same stage, the increase in size of morphant optic vesicles was also apparent (Figs. 6A and B). We therefore determined the average number of cells (Fig. 6E) and the mitotic indexes (Fig. 6G) for morphant and control embryos in the optic vesicles. Loss of *lmo4b* resulted in a significant increase in the total cell number in the optic vesicles ($p=1.5\times10^{-6}$). We did not observe a statistically significant increase in the mitotic index ($p=0.2$). We cannot rule out small changes in the rate of cell proliferation, which are not directly measured in these experiments, or a more significant change in the mitotic index at other stages. However, our data are consistent with the possibility that any changes in cell cycle parameters that may occur in the absence of *lmo4b* are mediated by the resultant increases in *six3b* and *rx3* expression. Thus, the increase in size of the optic and telencephalic primordia might result from both increased recruitment of cells into the anterior neuroectoderm by persistent *six3b* expression, followed by expansion of the anterior neuroectoderm through Six3- and Rx3-dependent proliferation.

Overexpression of *lmo4b* decreases the size of the telencephalon, eyes and hypothalamus

The decrease in the *six3b*, *rx3* and *zic1* expression domains observed when *lmo4b* is overexpressed supports the hypothesis that *lmo4b* functions to limit forebrain and eye specification and growth. We confirmed this hypothesis with a detailed characterization of eye and forebrain development in embryos overexpressing *lmo4b*. Global misexpression by injection of mRNA at the 1–4 cell stage strongly suppressed eye development, but had an apparently smaller effect on telencephalic and hypothalamic development. At 3 dpf (Figs. 7A and B), larvae were similar to wild type or control injections in size and gross morphology, though the vast majority of larvae lacked eyes or had only rudimentary eyes (Fig. 7B), with

apparently more preoptic tissue. This phenotype is superficially similar to *chokh* mutant larvae, in which the *rx3* gene is inactivated by mutation (Kennedy et al., 2004; Loosli et al., 2003; Rojas-Munoz et al., 2005; Stigloher et al., 2006). We therefore wished to characterize the effects of *lmo4b* expression on the eye and telencephalon in more detail.

We first noted that the anterior neural plate, as revealed by *dlx3* and *pax2a* expression, was smaller along its anterioposterior dimension (Figs. 7C and D) in *lmo4b*-overexpressing embryos by 1s stage. Measurements of the width of the *pax2a* stripe did not reveal significant differences between injected and control embryos (not shown), again suggesting that the relevant targets of *lmo4b* are anterior to the MHB. Expression of *emx1* and *pax6b* revealed the presence of both telencephalic and optic primordia at the 1s stage, in shorter and narrower domains than seen in control embryos (Figs. 7E and F). The presumptive telencephalon of overexpressing embryos is shorter than that of control embryos after neurulation (Figs. 7G and H).

At 24 hpf, the region anterior to the zona limitans intrathalamica (ZLI in Figs. 7I and J), marked by *shh* expression, is smaller in overexpressing embryos, as is the *shh* expression domain in the hypothalamus (h in Figs. 7I and J). Telencephalic (t in Figs. 7I and J) and preoptic tissue, while reduced relative to control embryos, appear less strongly affected than the optic primordia by *lmo4b* overexpression. The difference in the size of the hypothalamus, stained for expression of *nk2.1a*, is shown in ventral view in Figures 7M and N.

Gene expression analysis and morphological observation suggested that overexpression of *lmo4b* impairs the specification of the eye field and expansion of the optic vesicles, but not the evagination of the vesicles or the differentiation of cell types within the optic vesicles. At the 8s stage, bilateral vesicles that express *pax6b* are present (Figs. 7E and F). These vesicles are clearly separated from the neural tube by the 18s stage, where they also express *rx2*, a marker for differentiating retinal cells (Chuang et al., 1999; Chuang and Raymond, 2001; Kennedy et al., 2004; Rojas-Munoz et al., 2005) (Figs. 7G and H). This observation distinguishes *lmo4b*-overexpressing embryos from zebrafish *chokh* mutants and medaka eyeless (*el*) mutants, in which *rx2*-expressing cells remain medial (Rojas-Munoz et al., 2005; Winkler et al., 2000), reflecting a requirement for *rx3* function in directing cell behavior during optic vesicle evagination (Rembold et al., 2006). Similarly, in medaka *six3* morphant embryos, *rx2*-expressing cells fail to segregate to bilateral domains (Carl et al., 2002). As *lmo4b* overexpression does not completely ablate expression of *six3* or *rx3*, we conclude that the remaining *six3*- and *rx3*-expressing cells retain normal patterning and morphogenetic behavior.

Genetic interactions between *six3* and *lmo4* determine anterior neural tissue size and regional subdivision

Our results are consistent with the hypothesis that negative regulation of *six3b* expression is a primary function of Lmo4b. To test this hypothesis, we altered Six3b levels in *lmo4b* overexpressing embryos by co-injection of six3b morpholinos or mRNA. We first determined whether *lmo4b* gain of function phenotype could be modified by reduction in *six3b* function. If Lmo4b functions primarily to reduce *six3b* function in the anterior neuroectoderm, then the telencephalic and eye reduction caused by loss of *lmo4b* should be enhanced by reduction in *six3b* function. For *six3* morpholino experiments, we used a morpholino that is expected to block translation of both the *six3*a and *six3b* genes (Ando et al., 2005). Injection of 125pg of *lmo4b* mRNA resulted in a minor reduction of the forebrain and eyes (Figs. 8A and D). Similarly, embryos injected with 8pg of the *six3*a/*six3b* MO had only modest effects on eye and forebrain size (Figs. 8B and E). However, co-injection of 125pg of *lmo4b* mRNA with 8pg *six3b* MO resulted in a severe reduction of forebrain and especially the eye (Figs. 8C and F). This result strengthens the conclusion that *lmo4b* exerts its effects at least in part through reduction of *six3b* activity.

We then tested whether elevation of *six3b* activity could compensate for reduction of eyes and forebrain resulting from overexpression of high levels (750pg) of *lmo4b* (Fig. 7). If *six3b* is inhibited transcriptionally by *lmo4b*, then injecting *six3b* mRNA should generate Six3b activity in an Lmo4b-independent manner, and thus suppress any aspects of the *lmo4b* overexpression phenotype resulting from transcriptional inhibition of *six3b*. This experiment allows us to distinguish effects of altered *lmo4b* function that are dependent on *six3b* transcription from those that are dependent on transcription of downstream or parallel genes. Injection of 40pg of *six3b* mRNA increased the size of the head and the eye (Figs. 8G), while injection of 750pg of *lmo4b* mRNA has the opposite effect (Fig. 7, Figs. 8H). Co-injection of both mRNAs resulted in embryos with enlarged heads but very small eyes at the 28hpf (Figs. 8I). The effects of these manipulation on the telencephalic primordia (*emx1* positive, dark blue in Fig. 8J–L) and optic vesicles (*pax6* positive, light blue in Fig. 8J–L) are apparent at the 10s stage (Fig. 8J–L). Thus, overexpression of *six3b* can overcome the decrease in forebrain size caused by *lmo4b* overexpression, but not the decrease in optic primordia size. This suggests that *lmo4b* negatively regulates other eye field genes, independently of its effect on *six3b* transcription.

To examine this further, we looked for the ability of *lmo4b* overexpression to uncouple expansion of the eye field from expansion of the anterior neural plate induced by co-injection of *six3b*. We have shown that *lmo4b* overexpression decreases the size of the neural plate (Fig. 7D), and eye field (Figs. 5I and J; Fig. 7F) while other studies (Ando et al., 2005; Andreazzoli et al., 2003;Kobayashi et al., 1998;Lagutin et al., 2003;Loosli et al., 1999) have shown that overexpression of *six3b* has the opposite effect. Here we show that in co-overexpressing embryos, the *six3b* gain of function phenotype (Fig. 8M) dominates with respect to the size of the anterior neural plate (Fig. 8O), as marked by *dlx3* expression at the neural boundary, but not the eye field as marked by *rx3* expression (Fig. 8M–O). We conclude that negative regulation of *rx3* by Lmo4b is independent of the effects of Lmo4b on *six3b* transcription, while positioning of the anterior neural boundary by *lmo4b* is mediated by transcriptional regulation of *six3b*.

Discussion

We have identified the zebrafish *lmo4b* gene as an essential negative regulator of specification and growth in the telencephalon and eye. We have characterized two distinct phases of *lmo4b* expression, at the anterior neural boundary after bud stage, and in the presumptive telencephalon and eye after the 3s stage, which most likely account for its activity in anterior neural development. We have identified *six3b* and *rx3*, known regulators of specification and proliferation of forebrain and eye tissue, as independent downstream effectors of *lmo4b* activity in anterior neural tissue. Our results demonstrate the importance of *lmo4b* in stabilizing the anterior neural boundary immediately after gastrulation and in restricting the size of the presumptive forebrain and eyes. Importantly, our results indicate that vertebrate Lmo4 is not a dedicated cell proliferation factor, as studies in cultured cells, mammary tumors and mammalian embryos have suggested.

Two phases of *lmo4b* function in anterior neural development

We propose that the *lmo4b* morphant phenotype that we describe here reflects a requirement for Lmo4b activity in two important aspects of early forebrain and eye development. We show that *lmo4b* is first expressed in the anterior neural boundary region during the late bud-3s stage, and initially overlaps with expression of *zic1* (Figs. 4D and E) and *six3b* (not shown) before being segregated to the non-neural ectoderm (Fig. 4G). We propose that *lmo4b* activity is required to attenuate expression of neural genes in the presumptive neural boundary, thus restricting the number of cells that become committed to a neural fate. In support of this hypothesis, elevated levels of *lmo4b* cannot interfere with the ability of ectopic *six3b* to expand

the neural plate, suggesting that transcriptional repression of *six3b* is central to the function of *lmo4b* at the boundary. This implies some plasticity in the boundary at the bud-1s stages, and suggests that *lmo4b* is required only for the precise positioning of the boundary, rather than being required for boundary formation itself. In support of this, *dlx3* expression remains in morphant embryos (not shown) and placode-derived structures are present in morphant embryos (not shown).

Our results are consistent with the possibility that following boundary formation, *lmo4b* is required in neural tissue to modulate expression of genes, including *six3* and *rx3*, that maintain the high proliferation state of anterior neural cells during the pre-neurogenic expansion period. This proposed second phase of *lmo4b* function follows from the observation that *lmo4b* expression is maintained throughout the neural tissue during and after the 6s stage, and that elevated *lmo4b* activity inhibits Six3-dependent *rx3* expression. *rx3* is required for evagination and expansion of the optic vesicles (Kennedy et al., 2004; Loosli et al., 2003; Loosli et al., 2001; Rembold et al., 2006; Rojas-Munoz et al., 2005; Stigloher et al., 2006), and inhibition of *six3* function interferes with both of these processes (Carl et al., 2002; Lagutin et al., 2003), as well as with *rx3* expression (Carl et al., 2002). The demonstration that elevated *lmo4b* can suppress the effects of elevated *six3b* in the eye support our conclusion that *lmo4b* is required to limit *rx3* expression independently of its effect on *six3b* transcription, and may interfere with Six3b protein function, by direct interaction with Six3 or with other proteins that are regulated by Six3, in the maintenance of *rx3* expression. Modulation of *rx3* expression during expansion and evagination of the eye field and optic vesicles may serve to ensure timely mitotic exit and differentiation of neural precursor cells. This model is detailed in Figure 9. An alternative possibility is that both processes require different levels of *six3b* activity, and out experiments did not provide enough *six3b* to overcome the effects of lmo4b in the eye field.

Experiments in Drosophila and mammalian tissue culture indicate that LMO proteins act exclusively in the regulation of transcription by specific interactions with DNA-binding proteins. Our experiments have not addressed whether Lmo4b directly regulates transcription of *zic1*, *six3* or *rx3*. However, we detect the effects of loss of *lmo4b* function shortly after *lmo4b* expression in the anterior neural boundary region is initiated, indicating that regulation of early-expressed anterior neural genes is a proximal readout of Lmo4b activity. We note that we were unable suppress the *lmo4b* morphant phenotype by moderate reduction of *six3*a and *six3b* activity (not shown), suggesting that some of the effects of loss of *lmo4b* are independent of *six3*a and *six3b*. The existence of partially redundant genes, such as *six7* (Drivenes et al., 2000) or other early anterior neural genes that are regulated in parallel by Lmo4b could explain Six3-independent aspects of *lmo4b* function.

Lmo4b-dependent growth regulation of the hypothalamus

Our results show that the size of the hypothalamic primordia at 28 hpf is inversely correlated with *lmo4b* activity. A requirement for *six3* in regulation of specification or growth of the hypothalamus has not been reported, nor have we observed one in our experiments. In contrast, *rx3*, which is also a target of *lmo4b* negative regulation, is expressed in the presumptive hypothalamus, and loss of *rx3* results in an expansion of the hypothalamus, along with the telencephalon (Stigloher et al., 2006). However, the negative regulation of *rx3* by *lmo4b* is does not explain the effects of *lmo4b* on hypothalamus development, as this would predict a direct correlation between *lmo4b* activity and hypothalamic size. In addition, we do not see non-proportional changes in *rx3* expression in the hypothalamus in *lmo4b* morphants or overexpressing embryos (not shown). We consider it likely that the effect of *lmo4b* on the size of the hypothalamus is indirect. We note that *lmo4b* is also expressed in the anterior ventral midline tissue during segmentation (Lane et al., 2002), and this tissue is implicated in induction and patterning of the hypothalamus.

A novel role for LMO4

Mammalian LMO4 is expressed in highly proliferative cells of the mammary epithelium and the neural tube (Sum et al., 2005b), and loss of *Lmo4* activity by RNAi (Sum et al., 2005a) or genetic knockout (Lee et al., 2005; Tse et al., 2004) correlates with decreased proliferation in these tissues, leading to the suggestion that Lmo4 normally promotes cell proliferation. Our results indicate that zebrafish *Lmo4b* functions indirectly to limit cell proliferation in anterior neural tissue via negative regulation of *six3b* and *rx3* expression. We suggest that Lmo4 is not a dedicated proliferation factor, but that the effect on cell proliferation is context-dependent, and a function of the proteins that are regulated by Lmo4, by gene expression or protein-protein interactions. In support of this, a recent study by Setogawa et al. (Setogawa et al., 2006) shows that human Lmo4 can in some contexts induce the expression of p21 and thus inhibit cell proliferation.

We note differences between the *lmo4b* morphant phenotype and what has been described for the mouse LMO4 knockout, which shows embryonic or perinatal death, with neural tube defects including variable exencephaly and decreased cell proliferation in the anterior CNS. (Lee et al., 2005; Tse et al., 2004). In contrast, we do not observe exencephaly, and the enlarged neural tube and upregulation of *six3b* and *rx3* expression are consistent with the observed increase in the number of proliferating cells. There may be several explanations for this difference. It is possible that zebrafish *lmo4b* has a distinct function from mammalian *Lmo4* in anterior neural tissue, as teleosts have two *lmo4* genes that have diverged at the amino acid sequence level (Fig. 1A). The amino acid differences may confer functional differences, such as differences in affinity for interacting proteins. In addition, *lmo4a* and *lmo4b* have distinct expression patterns (S. Amin and M.E. Lane, in preparation). In contrast to mouse *Lmo4*, zebrafish *lmo4b* is not highly expressed in the proliferative ventricular zone throughout the neural tube (Lane et al., 2002). Although mammalian *Lmo4* is also expressed in anterior neural tissue (Lee et al., 2005), early expression of mammalian *Lmo4* at the anterior neural plate boundary has not been described. It is possible that, following duplication of the *lmo4* genes, *lmo4b* has acquired unique spatiotemporal regulation in anterior neural tissue. Given that LMO function depends entirely on the availability of factors with which it can interact, interspecies differences in spatiotemporal expression would be expected to have significant consequences for function.

However, an alternative possibility is that the underlying molecular mechanisms of *lmo4* function in anterior neural tissue are conserved between fish and mammals, but that compensation by the *lmo4a* co-ortholog in fish, as well as the structural and mechanical differences between mammalian and teleost forebrain developmental processes are responsible for the distinct phenotypic outcomes of loss of function. While many aspects of neural development are highly conserved among all vertebrates, this conservation does not include early determination of the anterior neural plate (Wilson and Houart, 2004), anterior neurulation mechanics (Hong and Brewster, 2006; Lowery and Sive, 2004) or the growth of the telencephalon relative to other regions of the brain (Wilson and Houart, 2004). Further refinement of the mammalian expression and phenotype, as well as analysis of the zebrafish *lmo4a*/*lmo4b* double knockdown, will be required to better understand the evolution of vertebrate Lmo4 and its developmental roles.

Acknowledgements

We thank Daniel Wagner, Lila Solnica-Krezel, Milan Jamrich, Jenya Grinblat and the Zebrafish International Resource Center for providing probes. We thank Soo Kwang Lee, Daniel Wagner, Mike Stern, Jenya Grinblat, Charles Sagerström, Derreth Phillips, and Damian Dalle Nogare for helpful comments on the manuscript. We are grateful to Eric Swindell, Mike Stern, and members of the Lane and Wagner labs for helpful discussions throughout the course of the work. The work was supported by a March of Dimes Basil O'Connor Starter Scholar Award to MEL, NIH grant R01 EY015305 to MEL, and NIH Biotechnology Training Grant to C. McCollum, and NSF IGERT training fellowship to S. Amin, and Houston Livestock and Rodeo Scholarship to C. McCollum and S. Amin. Finally, we are indebted to

the late Ronald W. Brannon, who provided outstanding fish care and laboratory support over the last five years. We dedicate this work to his memory.

References

Akimenko MA, Ekker M, Wegner J, Lin W, Westerfield M. Combinatorial expression of three zebrafish genes related to distal-less: part of a homeobox gene code for the head. J Neurosci 1994;14 :3475–86. [PubMed: 7911517]

Andoh H, Kobayashi M, Tsubokawa T, Uyemura K, Furuta T, Okamoto H. Lhx2 mediates the activity of Six3 in zebrafish forebrain growth. Dev Biol 2005;287:456–468. [PubMed: 16226737]

Andreazzoli M, Gestri G, Cremisi F, Casarosa S, Dawid IB, Barsacchi G. Xrx1 controls proliferation and neurogenesis in Xenopus anterior neural plate. Development 2003;130:5143–5154. [PubMed: 12975341]

Bailey TJ, El-Hodiri H, Zhang L, Shah R, Mathers PH, Jamrich M. Regulation of vertebrate eye development by Rx genes. Int J Dev Biol 2004;48:761–770. [PubMed: 15558469]

Carl M, Loosli F, Wittbrodt J. Six3 inactivation reveals its essential role for the formation and patterning of the vertebrate eye. Development 2002;129:4057–4063. [PubMed: 12163408]

Casarosa S, Amato MA, Andreazzoli M, Gestri G, Barsacchi G, Cremisi F. Xrx1 controls proliferation and multipotency of retinal progenitors. Mol Cell Neurosci 2003;22:25–36. [PubMed: 12595236]

Chuang JC, Mathers PH, Raymond PA. Expression of three Rx homeobox genes in embryonic and adult zebrafish. Mech Dev 1999;84:195–198. [PubMed: 10473141]

Chuang JC, Raymond PA. Zebrafish genes *rx1* and *rx2* help define the region of forebrain that gives rise to retina. Dev Biol 2001;231:13–30. [PubMed: 11180949]

Del Bene F, Tessmar-Raible K, Wittbrodt J. Direct interaction of geminin and Six3 in eye development. Nature 2004;427:745–749. [PubMed: 14973488]

Drivenes O, Seo HC, Fjose A. Characterisation of the promoter region of the zebrafish *six7* gene. Biochim Biophys Acta 2000;1491:240–247. [PubMed: 10760585]

Gestri G, Carl M, Appolloni I, Wilson SW, Barsacchi G, Andreazzoli M. Six3 functions in anterior neural plate specification by promoting cell proliferation and inhibiting Bmp4 expression. Development 2005;132:2401–2413. [PubMed: 15843413]

Grinblat Y, Gamse J, Patel M, Sive H. Determination of the zebrafish forebrain: induction and patterning. Development 1998;125:4403–16. [PubMed: 9778500]

Hahm K, Sum EY, Fujiwara Y, Lindeman GJ, Visvader JE, Orkin SH. Defective neural tube closure and anteroposterior patterning in mice lacking the LIM protein LMO4 or its interacting partner Deaf-1. Mol Cell Biol 2004;24:2074–2082. [PubMed: 14966286]

Hallonet M, Hollemann T, Pieler T, Gruss P. Vax1, a novel homeobox-containing gene, directs development of the basal forebrain and visual system. Genes Dev 1999;13:3106–14. [PubMed: 10601036]

Hong E, Brewster R. N-cadherin is required for the polarized cell behaviors that drive neurulation in the zebrafish. Development 2006;133:3895–3905. [PubMed: 16943271]

Hurtado R, Mikawa T. Enhanced sensitivity and stability in two-color in situ hybridization by means of a novel chromogenic substrate combination. Dev Dyn 2006;235:2811–2816. [PubMed: 16894600]

Kennedy BN, Stearns GW, Smyth VA, Ramamurthy V, van Eeden F, Ankoudinova I, Raible D, Hurley JB, Brockerhoff SE. Zebrafish *rx3* and *mab21l2* are required during eye morphogenesis. Dev Biol 2004;270:336–349. [PubMed: 15183718]

Kobayashi M, Nishikawa K, Suzuki T, Yamamoto M. The homeobox protein Six3 interacts with the Groucho corepressor and acts as a transcriptional repressor in eye and forebrain formation. Dev Biol 2001;232:315–326. [PubMed: 11401394]

Kobayashi M, Toyama R, Takeda H, Dawid IB, Kawakami K. Overexpression of the forebrain-specific homeobox gene *six3* induces rostral forebrain enlargement in zebrafish. Development 1998;125:2973–2982. [PubMed: 9655819]

Lagutin O, Zhu CC, Furuta Y, Rowitch DH, McMahon AP, Oliver G. Six3 promotes the formation of ectopic optic vesicle-like structures in mouse embryos. Dev Dyn 2001;221:342–349. [PubMed: 11458394]

Lagutin OV, Zhu CC, Kobayashi D, Topczewski J, Shimamura K, Puelles L, Russell HR, McKinnon PJ, Solnica-Krezel L, Oliver G. Six3 repression of Wnt signaling in the anterior neuroectoderm is essential for vertebrate forebrain development. Genes Dev 2003;17:368–379. [PubMed: 12569128]

Lane ME, Runko AP, Roy NM, Sagerstrom CG. Dynamic expression and regulation by Fgf8 and Pou2 of the zebrafish LIM-only gene, lmo4. Mech Dev 2002;119(Suppl 1):S185–189. [PubMed: 14516683]

Lee SK, Jurata LW, Nowak R, Lettieri K, Kenny DA, Pfaff SL, Gill GN. The LIM domain-only protein LMO4 is required for neural tube closure. Mol Cell Neurosci 2005;28:205–214. [PubMed: 15691703]

Loosli F, Staub W, Finger-Baier KC, Ober EA, Verkade H, Wittbrodt J, Baier H. Loss of eyes in zebrafish caused by mutation of *chokh/rx3*. EMBO Rep 2003;4:894–899. [PubMed: 12947416]

Loosli F, Winkler S, Burgtorf C, Wurmbach E, Ansorge W, Henrich T, Grabher C, Arendt D, Carl M, Krone A, et al. Medaka eyeless is the key factor linking retinal determination and eye growth. Development 2001;128:4035–4044. [PubMed: 11641226]

Loosli F, Winkler S, Wittbrodt J. Six3 overexpression initiates the formation of ectopic retina. Genes Dev 1999;13:649–654. [PubMed: 10090721]

Lopez-Rios J, Tessmar K, Loosli F, Wittbrodt J, Bovolenta P. Six3 and Six6 activity is modulated by members of the groucho family. Development 2003;130:185–195. [PubMed: 12441302]

Lowery LA, Sive H. Strategies of vertebrate neurulation and a reevaluation of teleost neural tube formation. Mech Dev 2004;121:1189–1197. [PubMed: 15327780]

Manetopoulos C, Hansson A, Karlsson J, Jonsson JI, Axelson H. The LIM-only protein LMO4 modulates the transcriptional activity of HEN1. Biochem Biophys Res Commun 2003;307:891–899. [PubMed: 12878195]

Mathers PH, Jamrich M. Regulation of eye formation by the Rx and pax6 homeobox genes. Cell Mol Life Sci 2000;57:186–194. [PubMed: 10766016]

Nornes S, Clarkson M, Mikkola I, Pedersen M, Bardsley A, Martinez JP, Krauss S, Johansen T. Zebrafish contains two *pax6* genes involved in eye development. Mech Dev 1998;77:185–96. [PubMed: 9831649]

Rembold M, Loosli F, Adams RJ, Wittbrodt J. Individual cell migration serves as the driving force for optic vesicle evagination. Science 2006;313:1130–1134. [PubMed: 16931763]

Rhinn M, Picker A, Brand M. Global and local mechanisms of forebrain and midbrain patterning. Curr Opin Neurobiol 2006;16:5–12. [PubMed: 16418000]

Rohr KB, Concha ML. Expression of *nk2.1a* during early development of the thyroid gland in zebrafish. Mech Dev 2000;95:267–270. [PubMed: 10906475]

Rojas-Munoz A, Dahm R, Nusslein-Volhard C. *chokh/rx3* specifies the retinal pigment epithelium fate independently of eye morphogenesis. Dev Biol 2005;288:348–362. [PubMed: 16300752]

Sagerstrom CG, Grinbalt Y, Sive H. Anteroposterior patterning in the zebrafish, Danio rerio: an explant assay reveals inductive and suppressive cell interactions. Development 1996;122:1873–83. [PubMed: 8674426]

Sagerstrom CG, Kao BA, Lane ME, Sive H. Isolation and characterization of posteriorly restricted genes in the zebrafish gastrula. Dev Dyn 2001;220:402–408. [PubMed: 11307172]

Setogawa T, Shinozaki-Yabana S, Masuda T, Matsuura K, Akiyama T. The tumor suppressor LKB1 induces p21 expression in collaboration with LMO4, GATA-6, and Ldb1. Biochem Biophys Res Commun 2006;343:1186–1190. [PubMed: 16580634]

Schauerte HE, van Eeden FJ, Fricke C, Odenthal J, Strahle U, Haffter P. Sonic hedgehog is not required for the induction of medial floor plate cells in the zebrafish. Development 1998;125:2983–93. [PubMed: 9655820]

Stigloher C, Ninkovic J, Laplante M, Geling A, Tannhauser B, Topp S, Kikuta H, Becker TS, Houart C, Bally-Cuif L. Segregation of telencephalic and eye-field identities inside the zebrafish forebrain territory is controlled by Rx3. Development 2006;133:2925–2935. [PubMed: 16818451]

Sum EY, O'Reilly LA, Jonas N, Lindeman GJ, Visvader JE. The LIM domain protein Lmo4 is highly expressed in proliferating mouse epithelial tissues. J Histochem Cytochem 2005a;53:475–486. [PubMed: 15805422]

Sum EY, Shackleton M, Hahm K, Thomas RM, O'Reilly LA, Wagner KU, Lindeman GJ, Visvader JE. Loss of the LIM domain protein Lmo4 in the mammary gland during pregnancy impedes lobuloalveolar development. Oncogene 2005b;24:4820–4828. [PubMed: 15856027]

Tse E, Smith AJ, Hunt S, Lavenir I, Forster A, Warren AJ, Grutz G, Foroni L, Carlton MB, Colledge WH, et al. Null mutation of the Lmo4 gene or a combined null mutation of the Lmo1/Lmo3 genes causes perinatal lethality, and Lmo4 controls neural tube development in mice. Mol Cell Biol 2004;24:2063–2073. [PubMed: 14966285]

Visvader JE, Venter D, Hahm K, Santamaria M, Sum EY, O'Reilly L, White D, Williams R, Armes J, Lindeman GJ. The LIM domain gene LMO4 inhibits differentiation of mammary epithelial cells in vitro and is overexpressed in breast cancer. Proc Natl Acad Sci U S A 2001;98:14452–14457. [PubMed: 11734645]

Wang N, Kudryavtseva E, Ch'en IL, McCormick J, Sugihara TM, Ruiz R, Andersen B. Expression of an engrailed-LMO4 fusion protein in mammary epithelial cells inhibits mammary gland development in mice. Oncogene 2004;23:1507–1513. [PubMed: 14676840]

Wilson SW, Houart C. Early steps in the development of the forebrain. Dev Cell 2004;6:167–181. [PubMed: 14960272]

Winkler S, Loosli F, Henrich T, Wakamatsu Y, Wittbrodt J. The conditional medaka mutation eyeless uncouples patterning and morphogenesis of the eye. Development 2000;127:1911–1919. [PubMed: 10751179]

Zuber ME, Gestri G, Viczian AS, Barsacchi G, Harris WA. Specification of the vertebrate eye by a network of eye field transcription factors. Development 2003;130:5155–5167. [PubMed: 12944429]

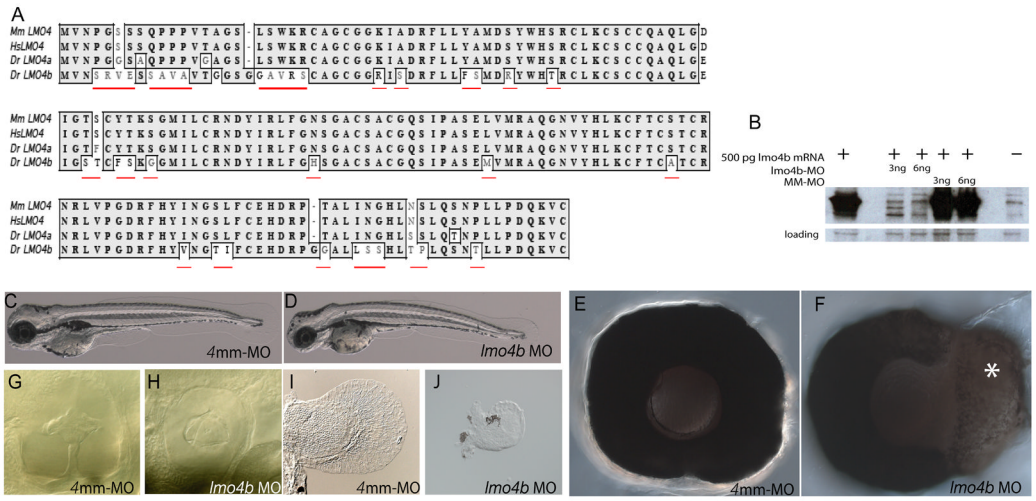

Figure 1. Zebrafish *lmo4b* is essential for viability and eye, ear and pectoral fin development

(A) Alignment of amino acid sequence alignment of zebrafish (Dr.) Lmo4b (Acc. #NP817093) with mouse (Mm.; Acc. #NM010723.1), human (Hs.; Acc. #NM006769.2) and zebrafish (Dr.) Lmo4a (Acc. #AAN03596). Residues unique to Lmo4b are underlined in red. (B) Western blot of extracts from embryos injected with 500pg of 6xmyc-*lmo4b* mRNA and a mixture of two non-overlapping translational-blocking MOs or a 4mm control MO, probed with anti-myc antibody. An unrelated immunoreactive band present in all extracts, demonstrates comparable loading for all lanes. (C–J) 72 hpf larvae or larval tissue from embryos injected with 4ng of either 4mm-MO (C, E, G, I) or 4ng of *lmo4b*-MO (D, F, H, J). High magnification views of morphant eyes reveal retinal enlargement (F) and defects in the ear (G, H) and pectoral fins (I, J).

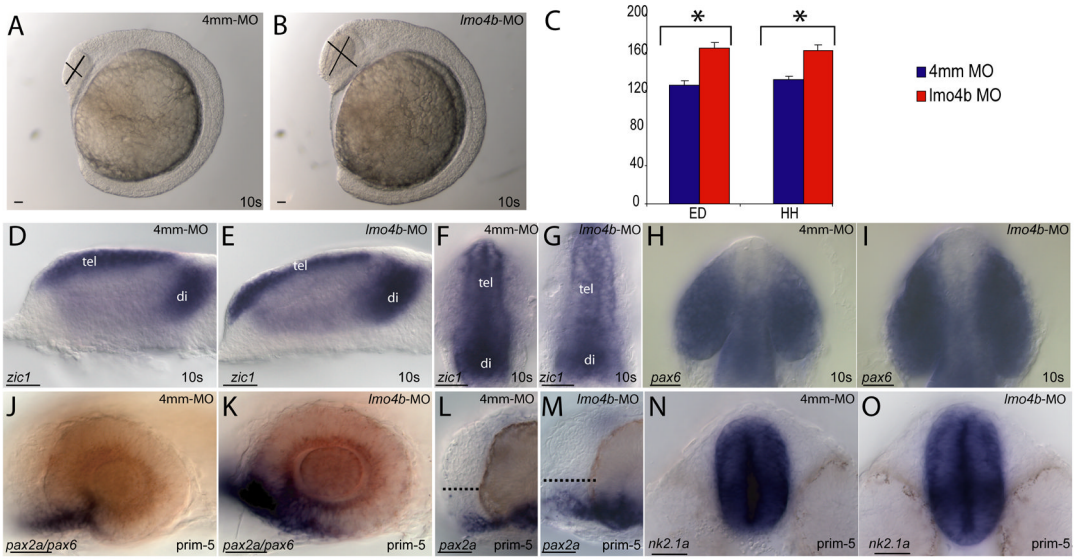

Figure 2. Loss of *lmo4b* causes forebrain and eye enlargement

(A, B) Lateral view of 10-somite embryos injected with 4ng of 4mm-MO (A) and 4ng of *lmo4b*-MO (B). (C) Quantitative representation of eye diameter (ED) and head height (HH) measurements of embryos injected with 4mm-MO (blue) and *lmo4b*-MO (red). Error bars represent standard error of the mean (SEM). Values in μ with confidence intervals for head height are 131±8 for control injections and 162±12 for morphants, and for eye diameter are 125±10 for control injections and 164±12 for morphants. For HH $p = 8.7\times10^{-5}$, for ED $p = 2.2\times10^{-5}$. (D–O) Whole mount views of embryos injected with 4mm-MO (D, F, H, J, L, N) and *lmo4b*-MO (E, G, I, K, M, O) show size differences in the forebrain and eyes. (D, E, and J–M) are lateral views. (F–I) are dorsal views of the anterior region, and (N, O) are ventral views of the anterior. The dashed lines in (L, M) represent pre-optic area. tel= telencephalon; di=diencephalon. Scale bars are 20μ.

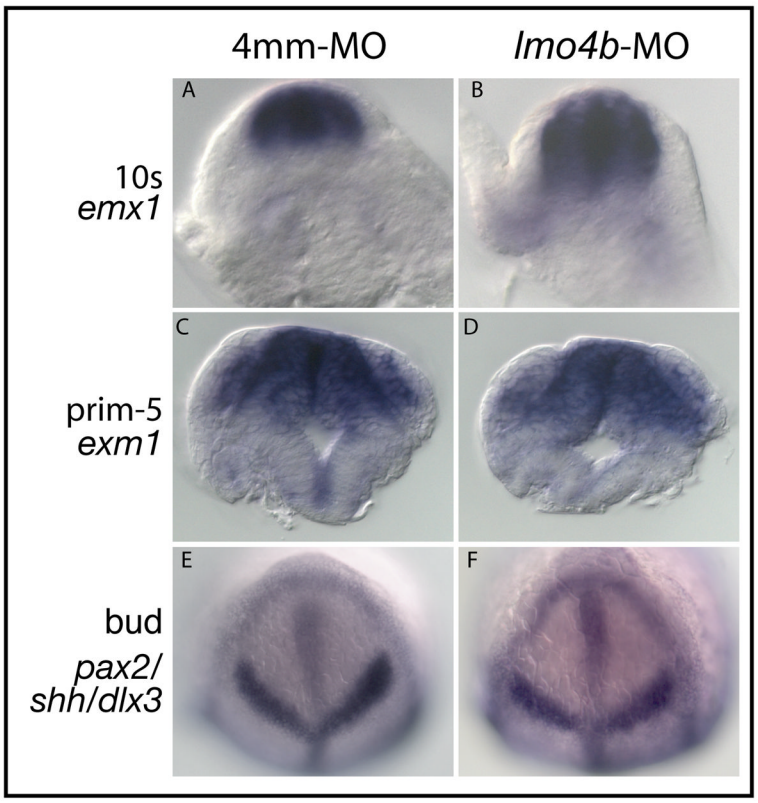

Figure 3. Neural tube closure and dorsoventral patterning are normal in *lmo4b* morphant embryos

(A–D) are cross sections through the anterior neural rod (A, B) or neural tube (C, D) in the region of the forebrain from control (A, C) and morphant (B, D) embryos. In situ hybridization probes used to localize forebrain tissue indicated at the left. (E, F) Bud stage embryos stained with probes to indicate the size of the anterior neural plate.

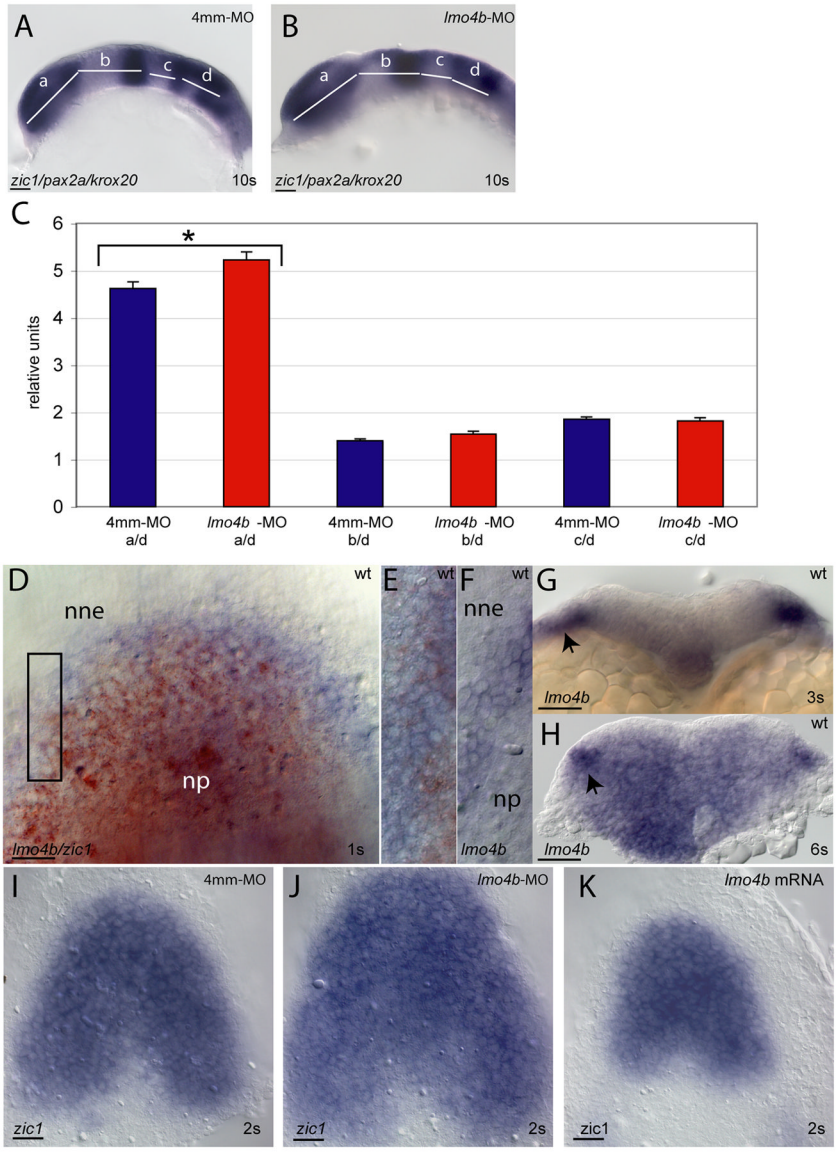

Figure 4. Loss of *lmo4b* expands the anterior neural plate

(A, B) Lateral views of embryos at the 10s stage stained with the regional markers *zic1*, *pax2a* and *krox20* to delineate regions that are measured and compared between control-injected (A) and morphant (B) embryos. (C) Measurements are normalized to the size of rhombomeres 3–5 (region **d**). Bars indicate standard error of the mean. Statistically significant differences are indicated with an asterisk. Individual values, with confidence intervals, for control (blue) and morphant (red) respectively are: a/d=4.6±0.3 and 5.2±0.3; b/d=1.4±0.1 and 1.5±0.1; c/d= 1.9±.01 and 1.8±0.1. *p* values are indicated in the text. (D–F) Dorsal views of the anterior neural plate of embryos at the 1s stage, stained for expression *lmo4b* (blue) and *zic1* (red) (D, E) or *lmo4b* alone (F) to mark the neural plate (np), neural boundary and non-neural ectoderm (nne). (E) is an enlargement of the region indicated by the box in (D) and (F) is a similarly enlarged region from a different embryo. (G, H) are cross-sections through the anterior neural region of wild type embryos at the 3s (G) and 6s (H) stages. Arrowheads indicate non-neural ectoderm. (I–K) are dorsal views of the anterior neural plate stained for *zic1*

expression in embryos injected with 4mm-MO (I), *lmo4b*-MO (J) or 750pg *lmo4b* mRNA (K) at the 2s stage. Scale bars are 20 μ.

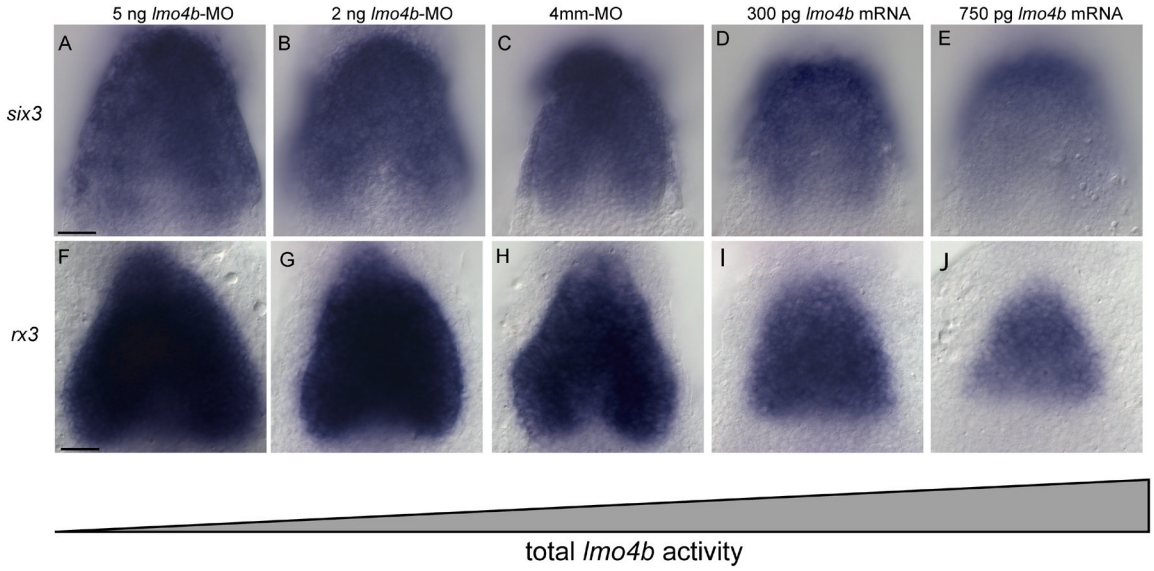

Figure 5. Dosage sensitive negative regulation of *six3* and *rx3* by *lmo4b*

All panels are dorsal view of the anterior neural region at the 3s stage. Embryos injected with *lmo4b* MO (A, B, F, G) control MO (C, H) or *lmo4b* mRNA (D, E, I, J) as labeled. Scale bars are 20 μ.

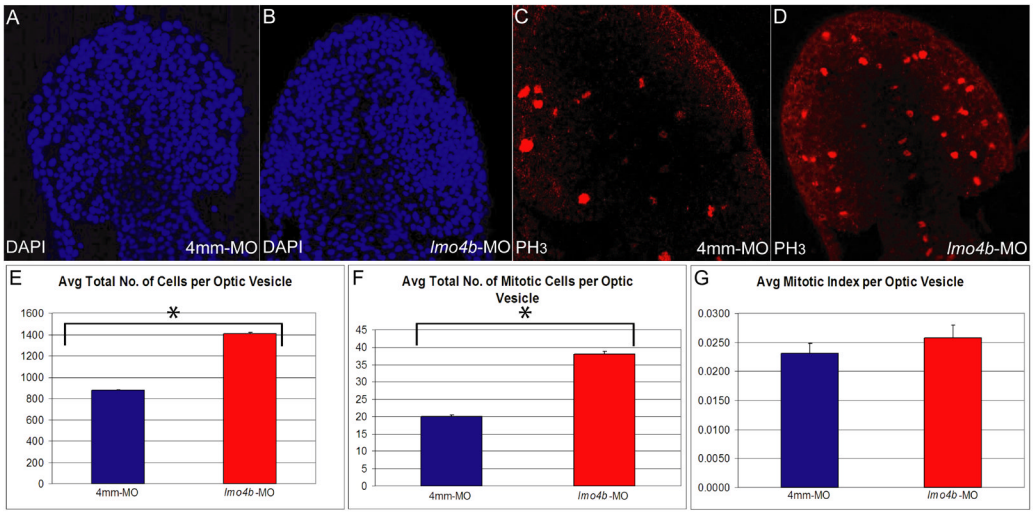

Figure 6. Loss of *lmo4b* results in higher average total cell nuclei and mitotic cell counts in the optic vesicle

(A–D) are dorsoanterior views of 7s stage embryos injected with 4ng of 4mm-MO (A, C) and 4ng of *lmo4b*-MO (B, D). (E–G) are graphical representations of average total cell nuclei count (E), average total mitotic cell count (F) and average mitotic index (G) per optic vesicle. Individual values with confidence intervals for control and morphants, respectively are: E=877 ±14 and 1410±30. F= 20 ± 1 and 58 ± 1. G=$2.3\times10^{-2} \pm 1.1\times10^{-3}$ and $2.6\times10^{-2} \pm 1.3\times10^{-3}$. *p* values are indicated in the text. n of *lmo4b* morphant optic vesicles = 13; n of control optic vesicles = 6. Error bars represent SEM.

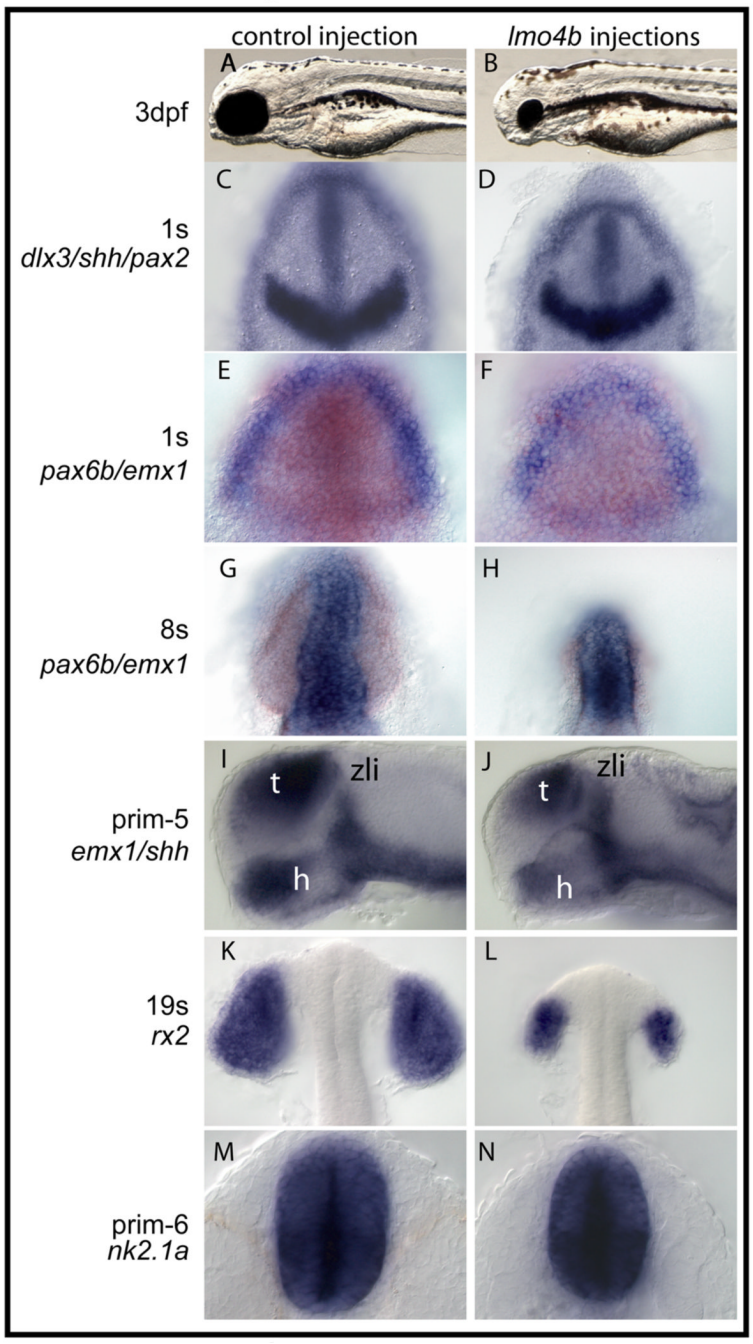

Figure 7. Overexpression of *lmo4b* reduces telencephalon and eye size

Embryos in the left were injected with 750 pg *gfp* mRNA, and embryos on the right were injected with 750 pg *lmo4b* mRNA. Probes and stages indicated on the far left. A, B. Lateral views of 3dpf larvae. (C–H, K, L) are dorsal views of the anterior region. In (E–H), *emx1* staining is blue and *pax6b* staining is orange. (I, J) are lateral views of the anterior region. (M, N) are ventral views. zli-zona limitans intrathalamica; h=hypothalamus. t=telencephalon.

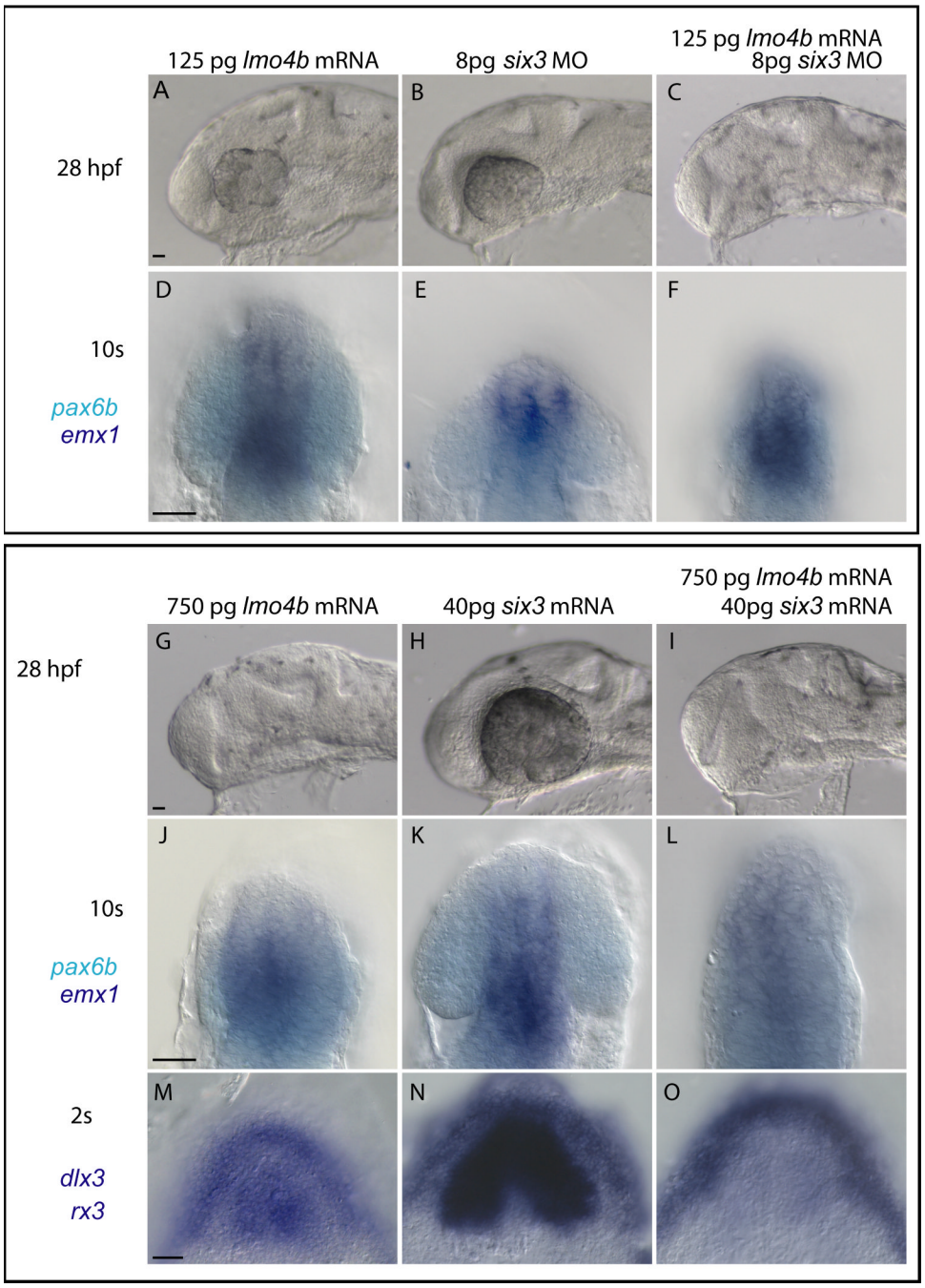

Figure 8. *lmo4b* overexpression modifies *six3* gain and loss of function phenotypes

Embryos injected with lmo4b mRNA and six3 MO (A–F) or six3b mRNA (G–O) as indicated in each panel, and stained by in situ hybridization as indicated in far left column. A–L are lateral views, D–F and J–L are enlarged views in a more superficial focal plane of the embryos in A–D and G–I, respectively. M–O are dorsal views of the anterior neural plate. Scale bar in all panels is 20μ.

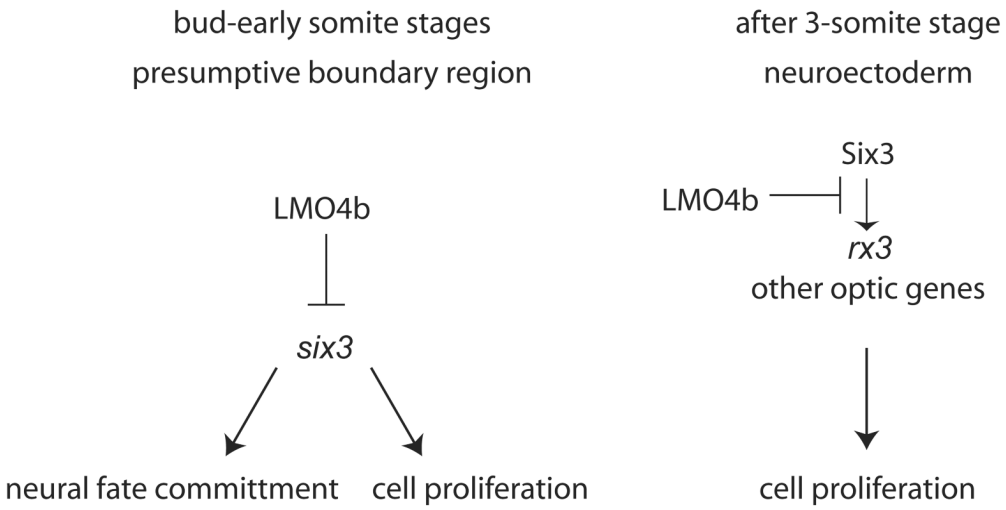

Figure 9. Model for LMO4b function in forebrain and eye development

Following gastrulation, Lmo4b in the presumptive neural boundary region negatively regulates transcription of *six3b* and limits commitment to neural fate. After the 3s stage, expression of Lmo4b throughout the anterior neuroectoderm limits the expression of *rx3* and perhaps other genes regulated by Six3, which ultimately limits cell proliferation. None of the arrows or inhibition bars are meant to imply direct protein-DNA or protein-protein interactions.